



Load-Capacity Evaluation of Polyacetal (POM) internal gears according to JIS B 1759:2016 (Effect of number of teeth of pinion)

I. Moriwaki¹ · K. Tatsuoka¹ · K. Kobayashi¹ · W. Nakamoto¹ · D. Iba¹ · A. Ueda²

Received: 23 March 2021 / Accepted: 3 November 2021 / Published online: 3 January 2022

© The Author(s), under exclusive licence to Springer-Verlag GmbH Deutschland, ein Teil von Springer Nature 2021

Abstract

The present paper describes the load capacity of POM internal gears, which were evaluated from the results of running tests according to JIS B 1759. As a result, POM internal gears showed a higher load capacity than expected from the running tests performed against external ones. The tendency became marked, especially on internal gears mating with a relatively large number of teeth steel pinion. Two indexes were proposed to explain the higher load capacity, i.e., the ratio of contact ratio for loaded teeth to geometrical one and an integral value of the PV. The contact ratio plays a fundamental role in estimating a load on one tooth, and the PV value indicates the frictional work, i.e., the tooth temperature during meshing. At present, however, only these indexes are not enough to explain the higher load capacity. Furthermore, cracks due to tooth-bending stress were observed to examine the 60°-tangent method for determining the critical-section position of internal gears. The observation demonstrated that the 30°- or 45°-tangent could be more suitable for the determination.

Tragfähigkeitsauswertung von Polyacetal (POM) Hohlrädern nach JIS B 1759:2016 (Auswirkung der Zähnezahls des Ritzels)

Zusammenfassung

Dieser Bericht beschreibt die Tragfähigkeit von POM-Hohlrädern, die aus den Ergebnissen von Lauftests nach JIS B 1759 bewertet wurden. Im Ergebnis zeigten POM-Hohlräder eine höhere Tragfähigkeit als aus den durchgeführten Lauftests gegen Außenräder zu erwarten war. Die Tendenz wurde deutlich, insbesondere bei Hohlrädern, die mit relativ vielen Zähnen aus Stahlritzeln zusammenpassen. Zwei Indizes wurden vorgeschlagen, um die höhere Tragfähigkeit zu erklären, d. h. das Verhältnis von Überdeckung für belastete Zähne zu geometrischer Eins und einem Integralwert des PV. Bei der Abschätzung der Belastung eines Zahnes spielt die Überdeckung eine fundamentale Rolle, und der PV-Wert gibt die Reibungsarbeit an, also die Zahntemperatur während des Eingriffs. Derzeit reichen jedoch allein diese Indizes nicht aus, um die höhere Tragfähigkeit zu erklären. Darüber hinaus wurden Risse aufgrund von Zahnfußspannungen beobachtet, um die 60°-Tangentenmethode zur Bestimmung der Position des kritischen Abschnitts von Hohlrädern zu untersuchen. Die Beobachtung zeigte, dass die 30°- oder 45°-Tangente für die Bestimmung besser geeignet sein könnte.

1 Introduction

An internal gear is one of the key elements for planetary-gear drives that realize compact units with high gear ra-

tios. In the future, primary movers would have higher rotation speed to permit higher torque to be obtained. Such systems require compact speed reducers with high gear ratios. Therefore, a planetary-gear drive is one of the leading candidates for such a reducer. An internal gear is the heaviest component in planetary gear drives, so that the replacement of internal-gear material from steel to plastics could cause considerable weight reduction.

In steel internal-gear pairs, the large tooth thickness of an internal gear provides lower tooth-root-bending stress than a pinion so that no breakage generally occurs at the tooth root of internal gears. Therefore, there are little research

✉ I. Moriwaki
ichi@mech.kit.ac.jp

¹ Kyoto Institute Of Technology, Matsugasaki, Sakyo-ku, Kyoto 606-8585, Japan

² AMTEC INC., Prior Tower 4305, Benten, Minato-ku, Osaka 552-0007, Japan

has been done on the bending-strength capacity of internal-gear teeth. Höhn et al. constructed back-to-back test rigs for internal gears and investigated their flank-load-carrying capacity [1], not bending-strength one. Sánchez et al. proposed a calculation method of tooth-bending strength and surface durability of internal spur gears [2] but performed no running tests. Singh et al. measured strains at internal-gear-tooth-root fillets [3] and discussed load sharing in a planetary-gear unit, not bending-strength capacity. ISO has published ISO 6336 series, which provides load-carrying-capacity calculations. The standard includes the calculation method of the bending-strength load capacity of internal-gear teeth [4]. However, there is little evidence that the proposed method has been thoroughly evaluated, possibly due to low demand for internal gears.

However, the mating of a steel pinion with a plastic internal gear could cause tooth breakage of an internal-gear tooth. Therefore, the bending-strength calculations would be one of the critical issues. Thus, a running-test rig for plastic internal gears was constructed for the bending-strength capacity to be evaluated.

In the present paper, the tooth-bending-strength capacity of POM internal gears are evaluated from running tests performed on the developed test rig according to JIS B 1759[5], “Estimation of tooth bending strength of cylindrical plastic gears.” Furthermore, this paper describes issues remaining in JIS B 1759 concerning the tooth-bending-strength estimation of internal gears.

2 Outline of JIS B 1759

Following ISO 6336-3:2019 [4], JIS B 1759 defines tooth bending stress, σ_F , as follows:

$$\sigma_F = \frac{F_{wt}}{b \cdot m_n} Y_F \cdot Y_S \cdot Y_\beta \cdot Y_f \cdot Y_B \quad (1)$$

where F_{wt} is a nominal tangential force on a working pitch circle, b is a facewidth, m_n is a normal module. Y_F , Y_S , Y_β , Y_f , and Y_B are a tooth form factor, a stress correction factor, a helix angle factor, a tooth fillet factor, and a rim thickness factor, respectively. ISO 6336 defines the nominal tangential force on the reference circle. The reference circle is related to individual gears, but load capacity should be evaluated for individual gear pairs. JIS B 1759, therefore, defines the nominal tangential force on the working pitch circle of the gear pair. Although the stress correction factor, Y_S , and the helix angle factor, Y_β , can be used directly from

ISO 6336-3, the tooth form factor, Y_F , must be modified as follows:

$$Y_F = \frac{\frac{6h_{Fe}}{m_n} \cos \alpha_{Fen}}{\left(\frac{s_{Fn}}{m_n}\right)^2 \cos \alpha_{wt}} \quad (2)$$

where h_{Fe} is a bending moment arm, s_{Fn} is a tooth root chord at the critical section, and α_{Fen} is a load direction angle. JIS B 1759 defines these quantities following ISO 6336-3.

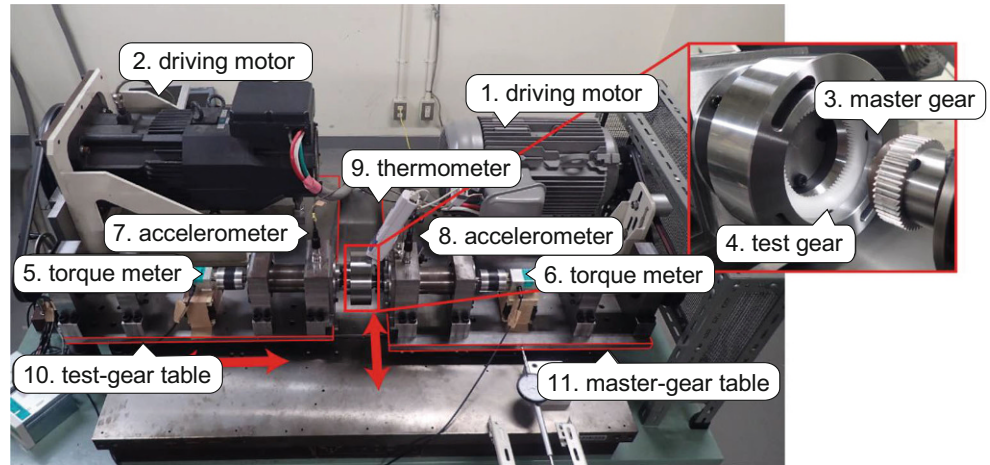
Because the nominal tangential force is determined at the working pitch circle, the working transverse pressure angle, α_{wt} , is used in Eq. 2 instead of the normal pressure angle, α_n , in ISO 6336-3. A reasonable alternative might be to use the transverse pressure angle, α_t , even when the nominal tangential force is defined on the reference circle. In either case, the difference in tooth form factors is within around 2% for helix angle less than 30 deg.

ISO 6336-3 has introduced the deep tooth factor, Y_{DT} , that is for high precision gears. Because of few precision plastic gears, at present, the factor would not be necessary for the load-capacity evaluation of plastic gears and has not been introduced into JIS B 1759.

Meanwhile, the general method for manufacturing plastic gears is injection molding, and a CAD/CAM system is usually used for manufacturing the mold. However, few CAD/CAM systems are equipped with a function for generating tooth-root fillets. Therefore, a mold designer who has little experience in gearing technology would design molds for plastic gears with a different fillet form, e.g., a single circular arc that many CAD/CAM systems can generate, from those defined by a standard basic rack. That could cause higher tooth root stress than expected. JIS B 1759 introduces the tooth fillet factor to adjust tooth root stress for such plastic gears. If a fillet has a standard form, $Y_f = 1.0$, otherwise $Y_f > 1.0$.

The rim thickness factor is significant for plastic gears. The smaller rim thickness could improve material flow into teeth and be effective for developing higher tooth-form accuracy. Therefore, the mold designers mentioned above would like to make rim thickness small. However, too small rim thickness affects stress distribution at tooth root to reduce load capacity. The rim thickness factor, therefore, has been introduced into ISO 6336-3. However, much lower stiffness of plastic than steel could make the rim-thickness effect on the load capacity more significant because of relatively larger strain. Thus the drafting committee for JIS B 1759 has determined the original factor based on run-

Fig. 1 KIT Running Test Rig for Plastic Gears [7]



ning tests and finite element analyses [6]. As a result, the rim thickness factor is given by

$$\left. \begin{aligned} Y_B &= 0.276 \ln \frac{52.9}{B_R} && \text{if } 0.4 \leq B_R \leq 1.4 \\ Y_B &= 1.0 && \text{if } 1.4 \leq B_R \end{aligned} \right\} \quad (3)$$

where B_R is a backup ratio that is the ratio of rim thickness to whole depth.

Although ISO 6336 has defined general influence factors, the drafting committee has thought these factors are unnecessary because plastics have a considerable running-in property and small weight. These properties could make the effects of uneven load distribution and dynamic load modest. Therefore, the committee decided not to introduce the general influence factors into JIS B 1759.

Meanwhile, JIS B 1759 defines a permissible tooth root bending stress, σ_{FP} , as follows:

$$\sigma_{FP} = \sigma_{Flim} \cdot Y_{NT} \cdot Y_\theta \cdot Y_{\Delta\theta} \cdot Y_L \cdot Y_M \quad (4)$$

where σ_{Flim} is a permissible bending stress of plastics as gear material, and Y_{NT} , Y_θ , $Y_{\Delta\theta}$, Y_L , and Y_M are a life factor, a temperature factor, a temperature-rise factor, a lubrication factor, and a mating-gear factor, respectively. The temperature factor, temperature-rise factor, lubrication factor, and mating-gear factor are newly introduced factors and provide for considering effects of ambient temperature, heat due to tooth-flank friction and hysteresis, lubricants, or material of mating gear, respectively.

Table 1 Specifications of the KIT Gear-Running-Test Rig

Max. power of driving motor kW	15
Max. torque applied to fest gear N · m	28.0
Max. rotation speed of fest gear min ⁻¹	5000
Center distance mm	0–100
Distance of gear shafts from table mm	115

In JIS B 1759, the permissible bending stress, σ_{Flim} , and the life factor, Y_{NT} , are determined from the results of running tests as follows: a) Running tests are performed under at least three different levels of applied torques at which tooth root fatigue breakage would occur before the meshing cycles of 10^6 . At least two tests must be carried out at each torque level. b) An S-N diagram is plotted from the results of running tests on a log-log chart. The ordinate of the diagram is the tooth root stresses calculated by Eq. 4, and the abscissa is the number, N , of cycles to failure. The straight line approximating these plots by the least square method is drawn and 2.33 σ lower to estimate the 90%-failure-probability value, where σ is the standard deviation of the plots from the approximate line. c) The tooth root stress at the point at which the shifted line intersects the line $N = 10^6$ is the permissible bending stress, σ_{Flim} . The life factor, Y_{NT} , is the normalized function of N representing the shifted line by the permissible bending stress.

3 KIT running-test rig for plastic gear

Fig. 1 shows the KIT (Kyoto Institute of Technology) running-test rig for plastic gears. This test rig is a power-absorption (open-power-circuit) type. JIS B 1759 recommends the power-absorption rig because tooth-flank wear could reduce an applied torque on a back-to-back test rig during the test, especially in the condition of no lubricants. The KIT gear-running-test rig permits either external or internal gears to be set with an appropriate jig. The close-up photograph in Fig. 1 shows an installation of internal test gear. Table 1 lists the specifications of the test rig.

The driving motor, ① (TFO-KK2P 15 kW, Hitachi Industrial Equipment Systems Co., Ltd.), drives a steel master gear, ③, which is a mating gear of plastic test gear, ④. Meanwhile, a braking motor, ② (HA-LFS152B, Mitsubishi Electric Corporation), applies torque to the test gear. These

Table 2 Gear Data

	Master gear	Test gear
Module mm	1.0	
Pres, angle deg	20.0	
Number of teeth	24, 48	67
Helix angle deg	0	0
Prof, shift coef	0	0
Facewidth mm	15.0	8.0
Tip diameter mm	26.0, 50.0	65.0
Root diameter mm	21.5, 45.5	69.5
Material	SCM420	POM

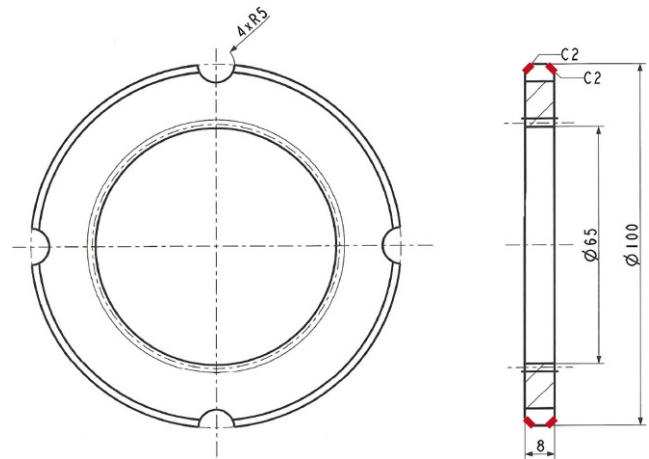


Fig. 2 Drawing of Test Gear [7]

Fig. 3 Drawing of Test-Gear-Mounting Jig [7]

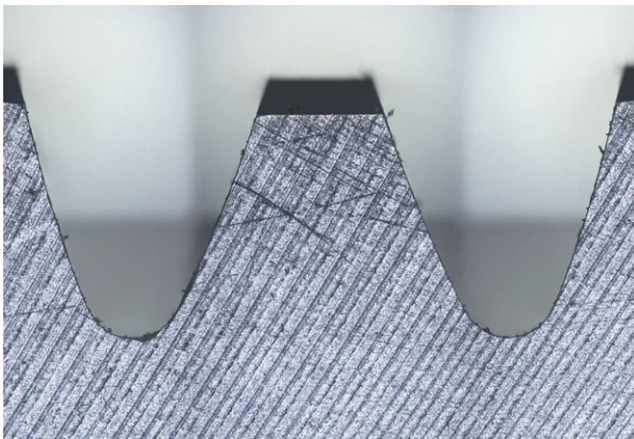
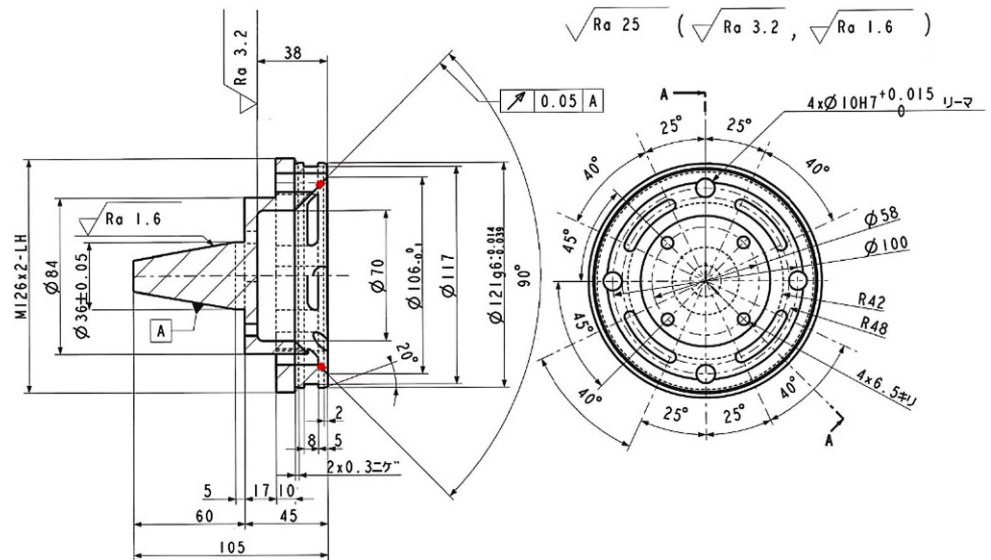


Fig. 4 Photograph of Test-Gear-Tooth-Root Fillet [7]

motors supply or absorb power via V-belts and pulleys. Torque meters, ⑤ & ⑥ (UTM-30N · m, UNIPULSE Corporation), are set between a pulley and test/master gear. These torque meters enable torque and rotation speed to be measured. Therefore, the torque meters can also measure the power loss between themselves. Accelerometers, ⑦ & ⑧ (NP-2810, ONO SOKKI Co., Ltd.), are set on the housings of gear-shaft bearings and allow gear-meshing vibrations to be measured. The data of input/output torques, rotation speeds, power losses, and gear vibrations are recorded on a PC via a data logger (WE7000, Yokogawa Electric Corporation) with a sampling frequency of 10kHz. The meshing-tooth temperature of test gear is one of the most critical data in running tests of plastic gears. However, it is impossible to measure it during running tests of internal gears. Therefore, an infrared thermometer, ⑨ (IT-550S, HORIBA, Ltd.), is set as shown in Fig. 1 to measure the temperature of a non-meshing tooth. In this setting,

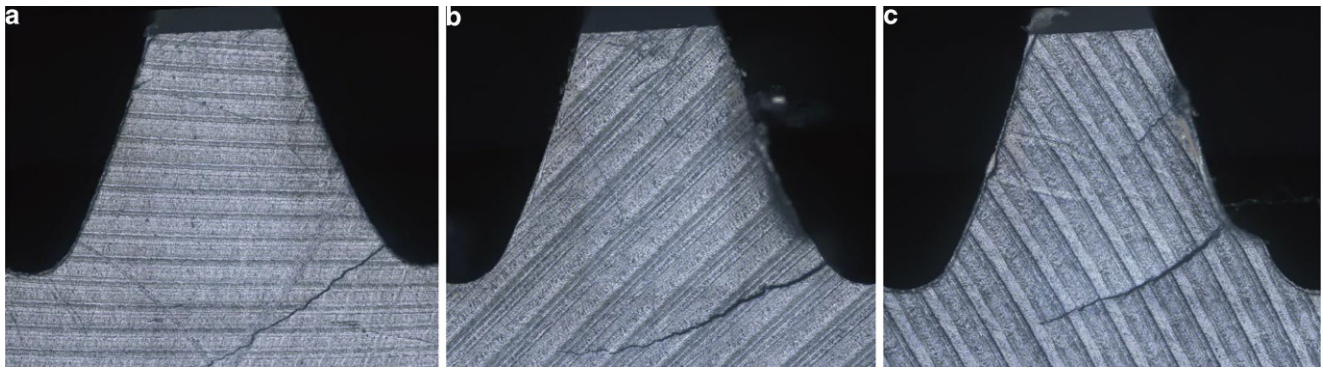


Fig. 5 Example Photographs of tooth root fatigue breakage. (a) $z_p = 48$, applied torque of $24 \text{ N} \cdot \text{m}$, (b) $z_p = 24$, applied torque of $14 \text{ N} \cdot \text{m}$, (c) $z_p = 24$, applied torque of $12 \text{ N} \cdot \text{m}$

the target point of measuring is on the side of the tooth 120° preceding the meshing tooth. The measured values are hereafter referred to as “preceding tooth temperature.” The preceding tooth temperature is also recorded on the PC via the data logger with a sampling frequency of 0.1 Hz.

The test-gear table, ⑩, on which a test gear, its shaft system, and the braking motor are placed, and the master-gear table, ⑪, on which a master gear, its shaft system, and the driving motor are positioned, can move in the directions shown in Fig. 1. These mechanisms permit the setting of test gears and the adjustment of center distance.

4 Test gear and master gear

Table 2 lists gear data of plastic-test gears and steel-master gears. Figs. 2 and 3 show drawings of the test gear and its mounting jig, respectively. The linear-expansion coefficient of plastics is around ten times larger than steel, which could cause a loose running fit for the test-gear and its mounting jig by heat due to gear meshing. The chamfers indicated red lines in Figs. 2 and 3 prevent the fit from being too loose.

As shown in Figs. 2 and 3, semi-circular projections of the jig mesh with grooves of the test gear to ensure the torque transmission. Test gears are made of extruded POM (M90-44, POLYPLASTICS CO., LTD.), and the teeth were cut using a pinion cutter with rounded tooth tips. Fig. 4 shows the photograph of the tooth-root fillet.

The test gears used in the present running tests are standard test gear so that $Y_f = 1.0$ and $Y_B = 1.0$. Therefore, tooth root stress can be calculated from

$$\sigma_F = \frac{F_{wt}}{b \cdot m_n} Y_F \cdot Y_S \cdot Y_\beta \tag{5}$$

5 Running tests

Before a running test, the specimens were cleaned for 5 min in acetone using an ultrasonic bath. The running test is

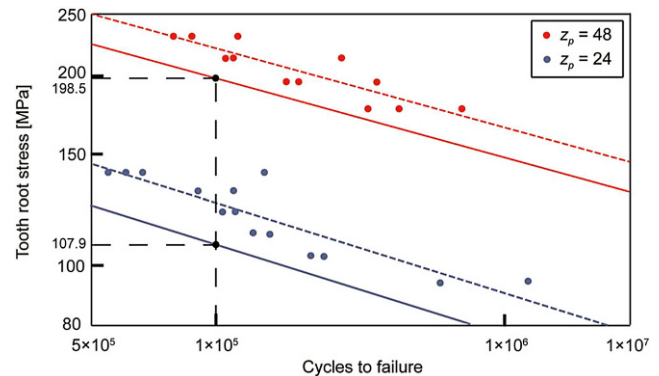


Fig. 6 S-N Diagram drawn according to JIS B 1759

carried out under a constant applied torque and rotation speed and continued until cracks at tooth-root fillets or tooth breakages occur. Monitoring the measured data, especially preceding tooth temperature, an operator judges whether a check on the test gear is necessary or not. If the operator would suppose cracks to nucleate, the operator stops the running test and checks visually whether cracks nucleated or not. If the operator finds some cracks, the operator finishes the test. If the operator does not find any cracks, the operator continues it. Table 3 lists the test conditions, where z_p is a number of teeth of a pinion.

Fig. 5 shows examples of tooth breakage after running tests. In most cases, a crack due to tooth bending occurred at the tooth fillet of a test gear as shown in Fig. 5a or b, but

Table 3 Test Conditions

	$Z_p = 24$	$Z_p = 48$
Rotation speed of test gear min^{-1}	1000	1000
Applied torque $\text{N} \cdot \text{m}$	10.0, 11.0, 12.0, 13.0, 14.0, 15.0	20.0, 22.0, 24.0, 26.0
Temperature $^\circ\text{C}$	23 ± 2	
Humidity %	50 ± 5	
Center distance mm	21.35	9.35

in rare cases, a test gear received cracks shown in Fig. 5c whose locations are different from the former ones. What could cause such a crack will be discussed later. In either case, all test gears showed tooth breakage at the end of a running test, so that it would be possible to evaluate these results according to JIS B 1759.

The present running tests were carried out under the standard test conditions define in JIS B 1759 so that factors Y_0 , $Y_{\Delta\theta}$, Y_L , and Y_M in Eq. 4 are unity. Therefore, a permissible tooth root bending stress can be calculated from

$$\sigma_{FP} = \sigma_{Flim} \cdot Y_{NT} \quad (6)$$

Fig. 6 shows the S-N diagram plotted the results of the present running tests. The KIT running-test rig has slightly insufficient power, which causes many plots in Fig. 6 to exceed $N = 10^6$.

Referring to Fig. 6, the permissible bending stresses are around 200MPa for $z_p = 48$ and about 110MPa for $z_p = 24$. The former is almost twice as large as the latter. In addition, the permissible bending stress evaluated from the results of running tests against external gears is about 80MPa [5]. This value is 40% of the estimation for $z_p = 48$. The large permissible bending stress will be discussed later.

Fig. 7 Tooth-flank-film elements. (a) internal gear pair (b) external gear pair

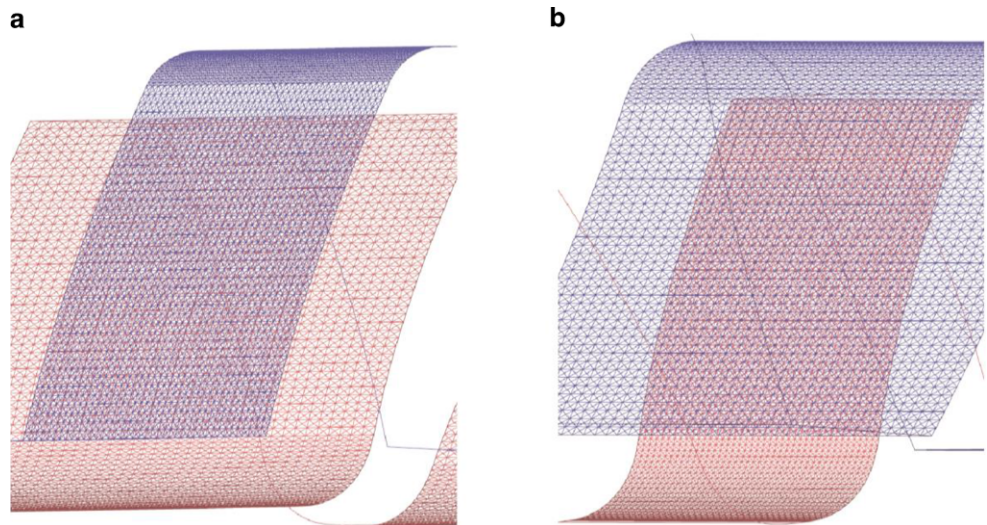
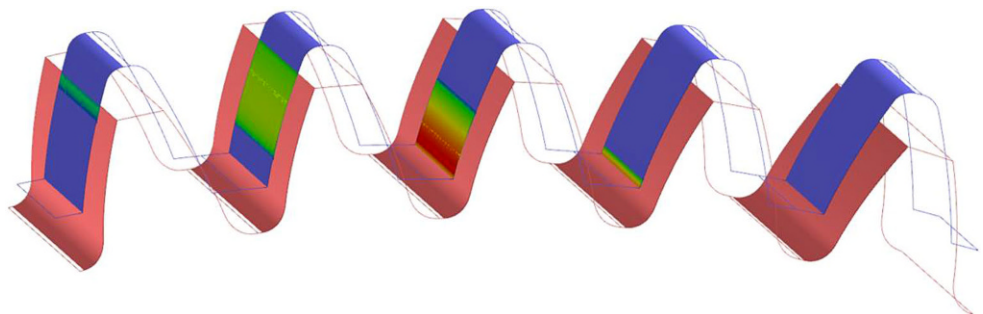


Fig. 8 Example of FEA Results (pinion number of teeth: 48; applied torque: 20N · m)



Meanwhile, the life factors are derived from the diagram as follows:

$$\left. \begin{aligned} Y_{NT} &= 12.25 N^{-0.181} && \text{for } z_p = 48 \\ Y_{NT} &= 17.32 N^{-0.206} && \text{for } z_p = 24 \end{aligned} \right\} \quad (7)$$

The power indexes are very similar so that the number of teeth of a pinion affects the fatigue property a lot less than the permissible bending stress.

6 Discussion on permissible bending stress

How can the differences between the evaluated permissible bending stresses be explained? Two possible answers could be offered: 1) The bending stress, σ_F , defined by Eq. 1 might be overestimated, 2) the temperature-rise factor in Eq. 5 might be greater than unity.

Lower bending stress might result from a relatively larger number of teeth meshing simultaneously than that calculated geometrically. Hasl et al. showed the effect of the actual contact ratio on tooth-bending stress of plastic gears and proposed “an appropriate ideal contact ratio factor” in ISO 6336-3[8]. However, it discussed external gears only. In order to examine the effect against internal gears, con-

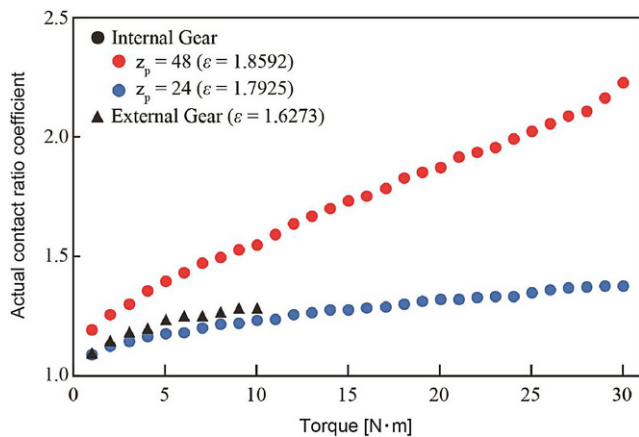


Fig. 9 Ratio of Contact-Ratio of Loaded Teeth to Geometrical One

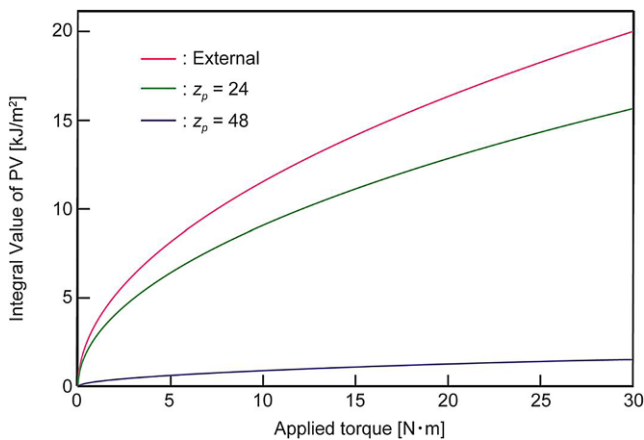


Fig. 10 Integral Values of PV along Line of Action

tact ratios of gear pairs transmitting torque were calculated with an FEA software for gearing, CTFEM Opera iii[9], Amtec Inc, which can facilitate contact problems appearing meshing gear teeth with tooth-flank-film elements[10]. The tooth-flank-film element is a virtual element placed on a tooth flank that enables a tooth contact area to be evaluated and contact stress distribution over the contact area to be calculated. Fig. 7 shows the tooth-flank-film elements used in the FEAs. Fig. 8 shows an example of the FEA results in which the steel pinion of $z_p = 48$ meshes with a POM internal gear at four teeth under the applied torque of $20\text{ N}\cdot\text{m}$.

The calculated contact ratio of statically loaded teeth is defined as follows: Angles, φ_S and φ_E , of a test gear are determined as a rotation angle at which a referred tooth starts and ends meshing through the FEAs at intervals of 0.05-deg rotation angle for one meshing pitch. The contact ratio, ε' , of loaded teeth is defined as

$$\varepsilon' = \frac{\Delta\varphi}{2\pi / z} \tag{8}$$

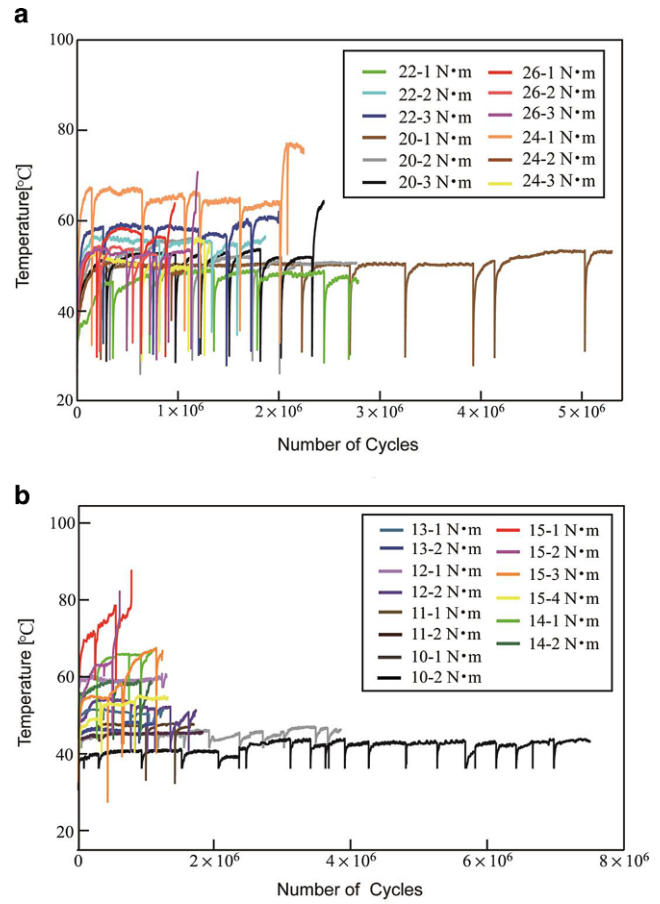


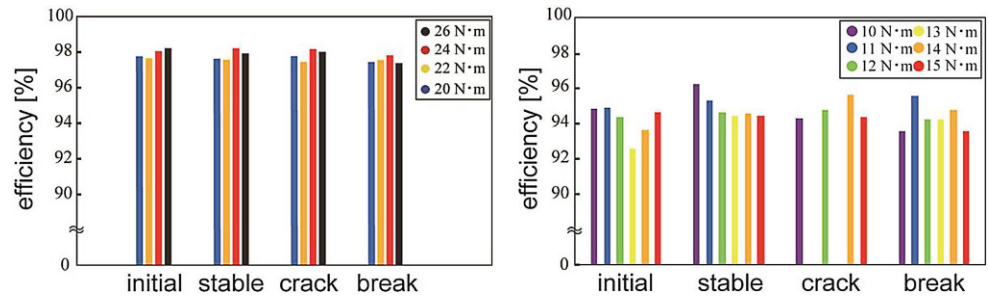
Fig. 11 Change in Measured Preceding Tooth Temperature (a) $z_p = 48$ (b) $z_p = 24$

where $\Delta\varphi = \varphi_E - \varphi_S$, and z is a number of teeth of a test gear.

Fig. 9 shows the change in calculated contact ratios with the increase of applied torques. For comparison, Fig. 9 also shows the change calculated in the case for an external gear pair consisting of a plastic test gear with 48 teeth and a steel master gear with 67 teeth [7]. Fig. 9 represents the ratio of the calculated contact ratio, ε' , of loaded teeth to the geometrical one, ε . Note that Young’s modulus of POM at room temperature was used in the FEAs, although tooth-flank sliding yields heat to increase tooth temperature.

Referring to Fig. 9, the ratio ε'/ε for $z_p = 48$ exceeds 1.8 under the applied torque of more than $20\text{ N}\cdot\text{m}$, while the ratio ε'/ε for $z_p = 24$ reaches around 1.2 under the applied torque of $12\text{ N}\cdot\text{m}$. The latter is not so different from the ratio ε'/ε for the external gear pair. Therefore, one of the main reasons internal gear pairs with more pinion teeth showed much higher permissible bending stress could be because a larger contact ratio of loaded teeth could be expected. However, internal gear pairs with fewer pinion teeth could be mainly affected by other factors.

Fig. 12 Measured Efficiencies
(a) $z_p = 48$ (b) $z_p = 24$



Internal gear pairs have a smaller sliding velocity between meshing tooth flanks than external ones because a pinion and internal gear have the same rotation direction. The smaller sliding could moderate the heat due to tooth-flank friction so that the temperature-rise factor in Eq. 5 would be greater than the value for external gears, i.e., unity.

Fig. 10 shows integral values, I_{PV} , of PV along the line of action, L , which is given by

$$I_{PV} = \int_L \frac{p_H \cdot v_t}{\omega \cdot d_b} dL \tag{9}$$

where p_H is Hertzian contact stress, v_t is sliding speed, ω is angular speed, and d_b is a base diameter of either pinion or gear, respectively. Equation 9 represents the time integral of PV value which means the work done by tangential force per unit area. If the friction coefficient would be constant over the tooth flank, the integral value times the friction coefficient corresponds to the frictional work done on a tooth during one meshing cycle. It follows that the integral value could be used as an index for evaluating the heat due to meshing and efficiency.

As shown in Fig. 10, the PV integral value for the external gear pair is around 10kJ under the applied torque of 5N·m. Meanwhile, the value for $z_p = 48$ is about 1kJ even under the greater applied torque of 20N·m. These two values have a considerable difference so that a temperature-rise factor for $z_p = 48$ could be much greater than unity.

That means much higher permissible tooth root bending stress. In contrast, the value for $z_p = 24$ is around 10kJ under the applied torque of 12N·m. This value is similar to that for the external gear pair mentioned above. Therefore, the measured preceding tooth temperature of $z_p = 48$ could be much lower than that of $z_p = 24$ which could make the measured efficiency of $z_p = 48$ much higher than that of $z_p = 24$. Fig. 11 shows the measured preceding tooth temperatures. Referring to Fig. 11, there is no clear trend between them. Fig. 12 shows the measured efficiencies evaluated from data obtained during 5 min of the initial, stable, and cracking periods. Unlike the measured temperatures, as shown in Fig. 11, the efficiency of $z_p = 48$ seems to be slightly higher than that of $z_p = 24$. However, that could be due to higher applied torque which means a large denominator in the efficiency equation. As a result, it was impossible to show the possibility of a higher temperature-rise factor from experimental data.

7 Discussion on location of critical section at tooth root

JIS B 1759 defines the tooth-root critical section, which is the crucial issue for evaluating tooth-root stress, according to the 60°-tangent method for internal gears, following ISO 6336-3. Referring again to the photographs in Fig. 5a and b, it seems that the tooth-root crack due to tooth bending

Fig. 13 Comparison between Methods for Determining Tooth-Root Critical Section. (a) $z_p = 48$, applied torque of 24N·m. (b) $z_p = 24$, applied torque of 14N·m

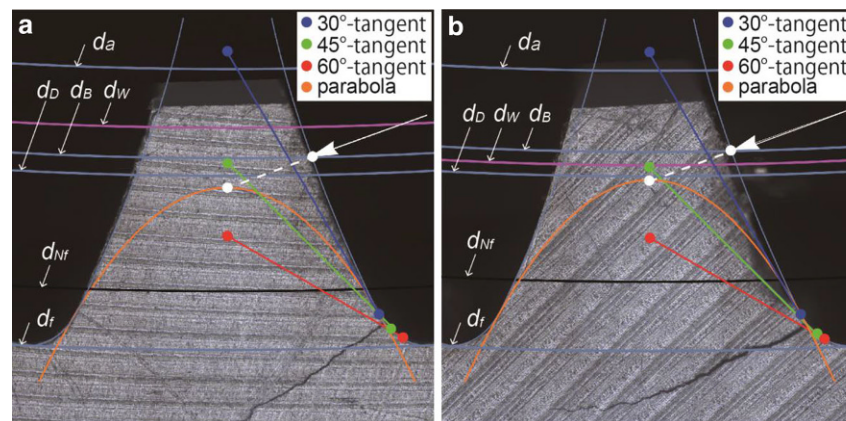


Table 4 Dimensions of Test-Gear Diameters

	Symbol	Master gear	Test gear
Tip diameter mm	d_a	26.0, 50.0	65.0
Root diameter mm	d_f	21.5, 45.5	69.5
Working pitch diameter mm	d_w	23.83, 48.13	66.53, 67.17
Active root diameter mm	d_{Nf}	22.68, 46.34	68.40, 68.54
Diameter of circle through the outer point of single-pair-tooth contact mm	d_B	24.02, 48.04	66.32, 66.43
Diameter of circle through the inner point of single-pair-tooth contact mm	d_D	23.62, 47.75	66.71

nucleated from the point that is different from the critical section defined in ISO 6336-3. Fig. 13 shows the calculated tooth profiles and tooth-root fillets, circles listed in Table 4, and inscribed parabolas, on which the Lewis formula for tooth-root stress is based, on the photographs of a tooth with the tooth-root crack. Fig. 13 also depicts 30°, 45°, and 60°-tangents for comparison. The 30°-tangent is used for determining the tooth-root critical section for external gears in ISO 6336-3, while the 45°-tangent was proposed as the determination method for internal gears by Oda and Miyachika [11]. Tooth-root fillets are subject to almost no plastic deformation so that it is easy to put tooth-root fillets on the photograph. After that, all the other items can be drawn on the photo referring to the fillets.

As shown in Fig. 13, the 30°-tangent touches with the tooth-root fillet at almost the same point as the inscribed parabola does. The location at which the tooth-root crack nucleated is between the contact points of the 30°- and the 45°-tangents with the tooth root fillet. Meanwhile, the 60°-tangent touches with the tooth-root fillet at the furthest point from the crack. Therefore, the 30°- or 45°-tangent method would be suitable at the very least for plastic internal gears instead of the 60°-tangent. At present, there is no way to calculate stress correction factors in the case of the 30°- or 45°-tangent method, so that the load capacity of POM

internal gears cannot be evaluated with the 30°- or 45°-tangent method. That must be one of the future discussions.

Referring to Fig. 13, the single-pair-tooth contact occurs in a small region whose size is comparable to a Hertzian contact width of tooth flanks. The region of the single-pair-tooth contact is determined geometrically under the assumption that tooth contact occurs not over an area but at a point. Therefore, the region that is comparable to the contact area could lead to no single-pair-tooth contact. That means double-pair teeth would contact over a whole tooth profile. As mentioned above, the actual number of teeth meshing simultaneously could be far greater. However, leaving aside that at the moment, the contact ratio is assumed to be two to determine the worst-loading point. Then, the worst-loading point could be on the tooth tip.

Fig. 14 shows the inscribed parabola drawn on the photograph in Fig. 5c under the assumption that the worst-loading point is on the tooth tip. Fig. 14 also shows the inscribed parabola based on the worst-loading position on the outer point of single-pair-tooth contact for comparison. As shown in Fig. 14, the inscribed parabola touches with the active tooth flank of a test gear near the center of tooth depth. But the location is slightly apart from that at which the crack on the tooth addendum nucleated. Therefore, the worst-loading point could not be on the tooth tip and be estimated considering the actual contact ratio.

The other crack at the tooth dedendum nucleated from the point through which the active root circle passes. That means the tooth tip of a mating steel gear could hardly collide with the location, so that tooth-flank wear could rapidly progress there. It follows that the hard collision could not just accelerate the wear but also initiate a crack.

8 Conclusions

The present paper described the load capacity of POM internal gears through running tests performed according to JIS B 1759. The results are summarized as follows:

1. POM internal gears have a higher load capacity than expected from running tests performed against external ones. The tendency becomes marked, especially on inter-

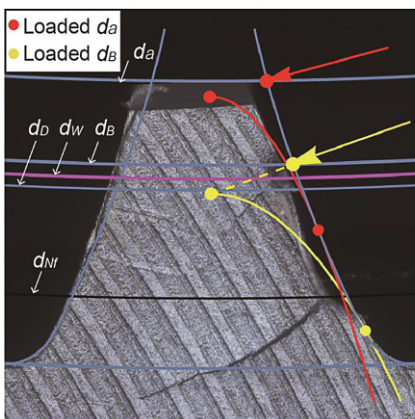


Fig. 14 Inscribed Parabola based on Worst-Loading-Point of Tooth Tip. ($z_p = 24$, applied torque of 12 N · m)

- nal gears mating with a relatively large number of teeth steel pinion.
2. The actual number of teeth meshing simultaneously is greater than the geometrical one in plastic internal gear pair because the lower Young's modulus causes large tooth deflections. That reduces tooth root stresses and increases load capacity. A new index would be proposed to represent the effect; i.e., the ratio of contact ratio for loaded teeth to the geometrical one.
 3. Another newly proposed index, an integral value of PV, showed the possibility of estimating the frictional work done on meshing teeth. However, the effect was hardly recognized through running tests.
 4. JIS B 1759 defines the tooth-root critical section according to the 60°-tangent method for internal gears, following ISO 633-3. However, cracks due to tooth bending nucleated at the point near the 30°- or 45°-tangent touching with the tooth-root fillet. At least for plastic internal gears, the 60°-tangent method could not be suitable for determining the critical section.

Acknowledgements The present study has been performed as a project supported by the JSPE technical committee on molded plastic gears. The authors extend sincere gratitude.

References

1. Höhn B-R, Stahl K, Schudy J, Tobie T, Zomek B (2012) FZG rig-based testing of flank load-carrying capacity internal gears. In: *GEARTECHNOLOGY* 06.2012, pp 60–69
2. Sánchez MB, Pleguezuelos M, Pedrero JI (2016) Calculation of tooth bending strength and surface durability of internal spur gear drives. *Mech Mach Theory* 95:102–113
3. Singh A, Kahraman A, Ligata H (2008) Internal gear strains and load sharing in planetary transmissions: model and experiments. *ASME J Mech Des.* <https://doi.org/10.1115/1.2890110>
4. ISO 6336-3:2019, Calculation of load capacity of spur and helical gears Part 3: Calculation of tooth bending strength.
5. JIS B 1759:2019, Estimation of tooth bending strength of cylindrical plastic gears (in Japanese).
6. Moriwaki I, Fukushima T, Ueda A, Nakamura M (2010) Effect of rim thickness on fatigue breakage in plastic-gear teeth. *J Japan Soc Precis Eng* 76(2):201–206 (in Japanese)
7. Moriwaki I, Murakami T, Tatsuoka K, Iba D, Ueda A (2019) Load capacity of Polyacetal POM internal gears. *J Japan Soc Precis Eng* 85(6):591–596 (Issues of JIS B 1759 appeared in running tests for internal gears (in Japanese))
8. Hasl C, Liu H, Oster P, Tobie T, Stahl K (2017) Method for calculating the tooth root stress of plastic spur gears meshing with steel gears under consideration of deflection-induced load sharing. *Mech Mach Theory* 111:152–163
9. Amtec Inc. <http://www.amtecinc.co.jp/new-catalogue/45.CT-FEM-Opera3.html>
10. Moriwaki I, Watanabe K, Nishiwaki I, Yatani K, Yoshihara M, Ueda A (2005) Finite element analysis of gear tooth stress with tooth flank film elements, proceedings of VDI international conference on gears. *VDI Ber* 1904(1):39–53
11. Oda S, Mitachika K (1985) Practical formula for true root stress of internal spur gear tooth (in Japanese). *Trans Japan Soc Mech Eng* 51(470):2720–2725 (Series C)